Conformational Studies of (±)-11,12-Didehydro-11-deoxycorynoline and (+)-11,13-Didehydro-11-deoxychelidonine, Hexahydrobenzo[*c*]phenanthridine-Type Alkaloid Derivatives, by X-Ray Crystal Structure and NMR Analyses

by **Miyoko Kamigauchi***[a]), **Yukiko Maekawa**[a]), **Chisato Tode**[a]), **Yasuko In**[b]), and **Toshimasa Ishida**[b])

[a]) Department of Physical Chemistry, Kobe Pharmaceutical University, 4-19-1 Motoyama-kitamachi, Higashinada-ku, Kobe 658-8558, Japan (phone: +81-78-441 7540; fax: +81-78-441 7541; e-mail: kamigami@kobepharma-u.ac.jp)

[b]) Osaka University of Pharmaceutical Sciences, 4-20-1 Nasahara, Takatsuki, Osaka 569-1094, Japan

The X-ray crystal analyses of the two 11-deoxy-didehydrohexahydrobenzo[*c*]phenanthridine-type alkaloid derivatives **3** and **4**, derived from (±)-corynoline (**1**) and (+)-chelidonine (**2**), established their structures as (±)-(5b*RS*,12b*RS*)-5b,12b,13,14-tetrahydro-5b,13-dimethyl[1,3]benzodioxolo[5,6-*c*]-1,3-dioxolo[4,5-*i*]phenanthridine (**3**) and (+)-*rel*-(12b*R*)-7,12b,13,14-tetrahydro-13-methyl[1,3]benzodioxolo[5,6-*c*]-1,3-dioxolo[4,5-*i*]phenanthridine (**4**). The conformations of **3** and **4** in $CDCl_3$ were determined on the basis of ^{1}H- and ^{13}C-NMR spectroscopy.

Introduction. – We have been investigating the relationship between structure and cell-adhesion-inhibitory activity of isoquinoline alkaloids [1][2]. Corynoline (**1**) [3] and chelidonine (**2**) [4], representative hexahydrobenzo[*c*]phenanthridine-type alkaloids [5], show a quite different activity for the cell-adhesion-inhibitory intensity [1], probably due to the presence or absence of the Me group at C(13)[1]). A similar deviation has been observed for the corresponding dehydrated compounds, *i.e.*, (±)-11,12-didehydro-11-deoxycorynoline[1]) (**3**) [6] and (+)-11,13-didehydro-11-deoxychelidonine[1]) (**4**) [7][8], where **3** shows an inhibitory activity of IC_{50} 166.0 μM which is slightly weaker than that of **1** (IC_{50} 54.8 μM) [1][2], while **4** exhibits no inhibitory activity at all. These compounds were prepared by dehydration of the OH–C(11) groups of **1** and **2** (*Fig. 1*).

The cell-adhesion-inhibitory effect could be due to an interaction of the inhibitor with the adhesive molecule [9], such as ICAM-1 [10][11], on blood-vessel epithelial cells. Thus, it is important to elucidate the conformational feature of the inhibitor for elucidating the structure–activity relationship. The chemical structures of **3** and **4** were determined by spectral methods [6–8], but their conformational features are still unknown. To compare these conformations with those of **1** and **2** and to further accumulate informations on the structure–activity relationship of hydrobenzo[*c*]phenanthridine-type alkaloids, we analyzed the solid-state and solution conformations of **3** and **4**.

Results and Discussion. – The crystallographic data of **3** and **4** are shown in *Table 1*. Selected bond lengths, bond angles, and torsion angles can be found in *Table 2*.

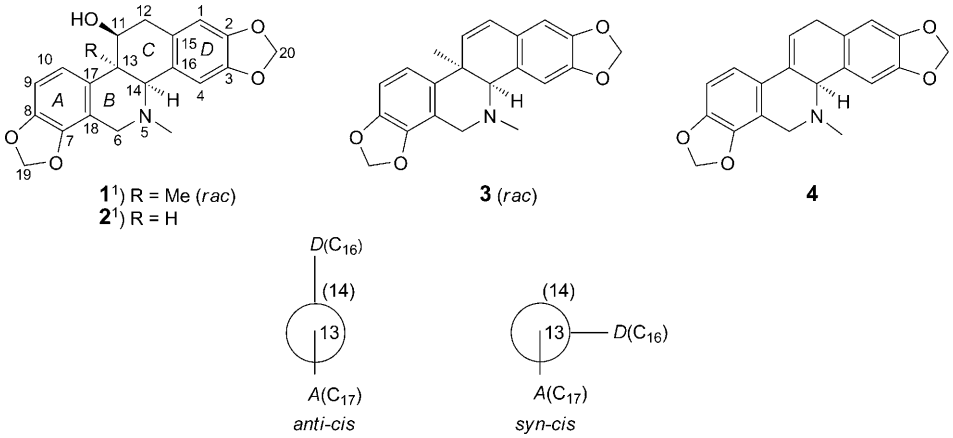

Fig. 1. *Structures of* **1**–**4**, *together with the atom numbering used in this work*[1]), *and* anti-cis *and* syn-cis *conformations illustrated by* Newman *projections viewed from C(13) to C(14) of the* B/C-cis-*fused hexahydrobenzo[*c*]phenanthridine skeleton*

The structure of **3** was determined by X-ray crystal analysis to be (±)-11,12-didehydro-11-deoxy-13-methylchelidonine (=(±)-(5b*RS*,12*RS*)-5b,12b,13,14-tetrahydro-5b,13-dimethyl[1,3]benzodioxolo[5,6-*c*]-1,3-dioxolo[4,5-*i*]phenanthridine), and that of **4** to be (+)-11,13-didehydro-11-deoxychelidonine (=(+)-*rel*-(12b*R*)-7,12b,13,14-tetrahydro-13-methyl[1,3]benzodioxolo[5,6-*c*]-1,3-dioxolo[4,5-*i*]phenanthridine). These structures support the structures deduced by chemical and spectroscopic methods. The conformations of **3** and **4** are shown in *Fig. 2*. Since the *cis*-fused *B*/*C*-ring juncture of the hexahydrobenzo[*c*]phenanthridine alkaloid is flexible, two types of conformers are possible, *i.e.*, the *anti* and *syn* type [12]. By looking down to C(13) from C(14) in the *Newman* projection, C(17) of ring *A* adopts either a τ of *ca.* 180° or *ca.* 90° with respect to C(16) of ring *D* for an *anti*-periplanar and *syn*-periplanar conformation, respectively (*Fig. 1*). However, the crystal structures show both the same *anti-cis B*/*C*-ring conformation with τ −171.0° for **3** and −174.8° for **4**. The ring-*B* conformations of **3** and **4** are half-chairs, and their *C* rings are almost planar due to the presence of two C=C bonds in this ring.

The dihedral angle between rings *A* and *D* in **3** is 62.3°. Although this value is slightly different from 46.79° in **1**, it is within the usual range of an alkaloid in the *anti*-type *B*/*C*-*cis*-ring conformation, and the relative positional relation of rings *A* and *D* in **3** is essentially the same as in **1**. The increased value of the dihedral angle of **3** by *ca.* 15° as compared with **1** could result from the lack of an intramolecular N(5)···HO–C(12) H-bond, which is present in **1** [14].

The dihedral angle between rings *A* and *D* in **4** is 15.3°, pointing to a rather planar shape of this partial structure. This value is in the same range as that of 14-epicorynoline (10.5°) [15], which has a *trans*-*B*/*C*-ring junction being an 14-epimer of **1**. The torsion angle C(11)–C(13)–C(14)–C(16) is 4.9(3)° for **4** and −50.3(2)° for **3**,

[1]) Trivial atom numbering; for systematic names of **3** and **4**, see *Exper. Part.*

Table 1. *Crystallographic Data of* **3** *and* **4**

	3	**4**
Crystallized from	$CHCl_3$/MeOH	acetone/MeOH
Empirical formula	$C_{21}H_{19}NO_4$	$C_{20}H_{17}NO_4$
M_r [g/mol]	349.37	335.35
Temperature [K]	120	120
Crystal system	monoclinic	orthorhombic
Space group	$P2_1/c$	$P2_12_12_1$
Z	4	4
θ Range for data collection [°]	1.99 – 28.26	1.87 – 28.23
Unit cell parameters:		
a [Å]	10.452(5)	6.2344(7)
b [Å]	12.839(5)	13.4636(16)
c [Å]	12.490(5)	18.588(2)
α [°]	90.000	90.000
β [°]	101.920(5)	90.000
γ [°]	90.000	90.000
V [Å^3]	1639.9(12)	1560.2(3)
$D_{calc.}$ [g/cm^{-3}]	1.4151	1.428
μ(MoK_α) [mm^{-1}]	0.098	0.100
F(000)	736	704
Radiation MoK_α λ [Å]	0.71073	0.71073
No. of reflections collected	10476	10060
No. of independent reflections	3894	3690
Data, restraints, parameters	3894, 0, 235	3690, 0, 226
Goodness-of-fit on F^2	1.138	1.160
R indices ($I > 2\sigma(I)$)	$R^1 = 0.0575$, $wR^2 = 0.1392$	$R^1 = 0.0517$, $wR^2 = 0.1249$
R indices (all data)	$R^1 = 0.0628$, $wR^2 = 0.1426$	$R^1 = 0.0538$, $wR^2 = 0.1262$
Δ_{max}/σ	0.000	0.000
$\Delta\rho$ (max; min) [e Å^{-3}]	0.397; −0.205	0.434; −0.258
Measurement	*Bruker SMART APEX*	*Bruker SMART APEX*
Program system	*Bruker SMART*	*Bruker SMART*
Structure determination	SIR92 [16]	SIR92 [16]
Refinement	full matrix SHELXL-97 [17]	full matrix SHELXL-97 [17]

indicating a notable difference. This difference is in part due to the planar shape of ring *C* in **4** but not in **3**. Also, the different direction of the Me–N(5) bond with respect to ring *B* would cause such a difference. The torsion angle C(22)–N(5)–C(14)–C(16) is −47.9(2)° in **3** due to the equatorial position of Me–N(5), similar to **1**, and the corresponding C(21)–N(5)–C(14)–C(16) is 69.2(2)° in **4** due to an axial Me–N bond, similar to 14-epicorynoline, endowed with a *trans-B*/*C*-ring juncture.

The conformations of **3** and **4** in solution were examined by NMR analyses (^{1}H at 499.7 and ^{13}C at 125.7 MHz). The ^{1}H- and ^{13}C-NMR data of **3** and **4** are given in *Tables 3* and *4*, respectively. In the NOESY plot of **3**, the two NOEs Me–N(5)/H–C(4) and H–C(10)/Me–C(13) are observed (*Fig. 3*,*a*), suggesting that the corresponding H-atoms are located in close vicinity; the X-ray distance between these H-atoms amounts to 2.91 and 2.15 Å, respectively. The NOESY plot of **4** shows a NOE H–C(10)/H–C(11) (*Fig. 3*,*b*), the distance between these H-atoms being 2.22 Å in the

Table 2. *Selected Bond Lengths, Bond Angles, and Torsion Angles of* **3** *and* **4**

Bond lengths [Å]	**3**	**4**
C(11)–C(12)	1.329(3)	1.495(3)
C(11)–C(13)	1.521(2)	1.334(3)
C(13)–C(14)	1.547(2)	1.520(3)
C(13)–C(21)	1.546(2)	–
N(5)–C(6)	1.460(2)	1.460(2)
N(5)–C(14)	1.478(2)	1.483(2)
Bond angles [°]	**3**	**4**
C(12)–C(11)–C(13)	122.0(2)	124.8(2)
C(11)–C(13)–C(14)	108.9(1)	121.7(2)
C(11)–C(13)–C(17)	109.7(1)	124.2(2)
C(11)–C(13)–C(21)	109.3(1)	–
C(13)–C(14)–N(5)	110.0 (1)	111.5(2)
C(16)–C(14)–C(13)	110.0(1)	114.8(2)
C(16)–C(14)–N(5)	110.5(1)	110.3(2)
C(6)–N(5)–C(14)	109.7(1)	109.3(2)
C(6)–N(5)–C(22)	108.3(1)	–
C(6)–N(5)–C(21)	–	110.9(2)
C(14)–N(5)–C(22)	113.6(1)	–
C(14)–N(5)–C(21)	–	112.6(2)
Torsion angles [°]	**3**	**4**
C(12)–C(11)–C(13)–C(14)	31.0(2)	4.1(3)
C(11)–C(13)–C(14)–N(5)	71.6(2)	131.3(2)
C(11)–C(13)–C(14)–C(16)	– 50.3(2)	4.9(3)
C(17)–C(13)–C(14)–N(5)	– 49.0(2)	– 48.4(2)
C(17)–C(13)–C(14)–C(16)	– 171.0(1)	– 174.8(2)
C(21)–C(13)–C(14)–C(16)	68.1(2)	–
C(21)–C(13)–C(14)–N(5)	– 169.9(1)	–
C(21)–N(5)–C(14)–C(16)	–	69.2(2)
C(22)–N(5)–C(14)–C(16)	– 47.9(2)	–

crystal structure. That is to say, the conformations of **3** and **4** estimated from the ^{1}H-NMR spectra agree well with the X-ray crystal structures.

In the *B*/*C-cis*-type hexahydrobenzo[*c*]phenanthridine-type alkaloids, the equatorial position of the Me–N group with respect to ring *B* could be energetically stable because the steric hindrance with the neighboring atom in the case of axial position is avoided [14]. Therefore, when the Me–N group is in axial position, a downfield shift by $\Delta\delta$ *ca.* 0.5 could be expected for H–C(4), as compared with the case of Me–N in equatorial position, due to the effect of the lone electron pair of the N-atom on the electron shielding of C(4). The chemical shift of H–C(4) of **4** (δ 7.173) is shifted by $\Delta\delta$ 0.4 towards lower field, as compared with that of **3** (δ 6.80). This explains that the axial Me–N(5) in **4** results from the avoidance of the steric interaction between Me–N(5) and H–C(4).

The C(4) signal of **4** in the ^{13}C-NMR spectrum is shifted to higher field ($\Delta\delta$ 4.3) compared to **3**. This is due to the effect on C(4) by the lone electron pair of N(5), when

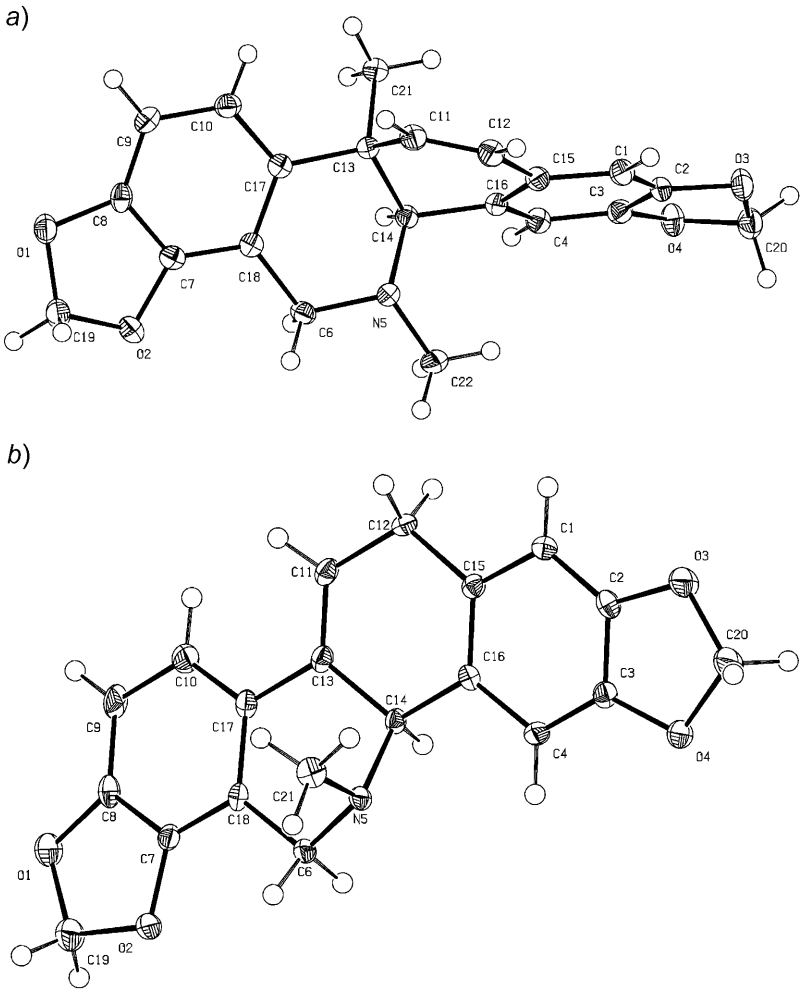

Fig. 2. ORTEP *Plots* [13] *of the molecular structures of* a) **3**[1]) *and* b) **4**[1]) (50% probability ellipsoids)

Me–N(5) is in axial position. The chemical shift values of C(10) and C(11) of **4** are at higher field by $\Delta\delta$ 3.5 and 18.8, respectively, than those of **3**. This could also be due to a *gauche* effect. In conclusion, both ^{13}C- and ^{1}H-NMR spectra show analogous tendencies concerning the conformational properties of **3** and **4**.

In summary, the present work established the most stable conformations of **3** and **4** in the crystal and solution states. The steric difference between the conformations of **3** and **4** could cause the different interaction with the adhesion protein ICAM-1, leading to the different inhibitory effects for cell adhesion.

Table 3. *^{1}H-NMR Data* (500 MHz, $CDCl_3$) *of* **3** *and* **4**[1]). δ in ppm, J in Hz.

	3	**4**
H–C(1)	6.62 (*s*)	6.60 (*s*)
H–C(4)	6.80 (*s*)	7.17 (*s*)
H–C(9)	6.79 (*d*, $J=8.0$)	6.74 (*d*, $J=8.3$)
H–C(10)	6.93 (*d*, $J=8.0$)	7.16 (*d*, $J=8.0$)
CH_2(6)	3.51 (*d*, $J=15.5$), 3.99 (*d*, $J=15.5$)	3.93 (*d*, $J=17.0$), 4.45 (*d*, $J=17.0$)
H–C(11)	5.83 (*dd*, $J=1.5$, 9.5)	6.50 (*m*)
H–C(12) or CH_2(12)	6.27 (*d*, $J=9.5$)	3.44 (*m*), 3.56 (*m*)
H–C(14)	3.19 (*s*)	4.56 (*m*)
Me–N(5)	2.12 (*s*)	2.00 (*s*)
Me–C(13)	1.25 (*s*)	–
CH_2(19), CH_2(20)	5.95 (*dd*, $J=13$, 1.5), 5.97 (*s*)	5.93 (*dd*, $J=9.5$, 1.5), 5.98 (*dd*, $J=9.5$, 1.5)

Table 4. *^{13}C-NMR Data of* **3** *and* **4** *at 125 MHz in $CDCl_3$*[1]). δ in ppm, J in Hz.

	3	**4**
C(21)	25.066	–
Me–N(5)	42.144	34.565
C(1)	106.610	106.914
C(4)	112.341	108.028
C(9)	106.536	106.892
C(10)	119.520	116.054
C(6)	52.947	51.966
C(11)	138.175	119.383
C(12)	123.725	30.463
C(13)	39.563	126.639
C(14)	69.873	58.130
C(19)	101.024	100.738
C(20)	101.186	101.286
C(15)	127.224	127.350
C(16)	126.221	127.350
C(17)	135.054	128.542
C(18)	116.425	114.650
C(2)	147.453	146.350
C(3)	146.168	146.657
C(7)	142.984	144.502
C(8)	144.858	146.820

Experimental Part

(±)-11,12-Didehydro-11-deoxycorynoline (=*(±)-(5b*RS*,12b*RS*)-5b,12b,13,14-Tetrahydro-5b,13-dimethyl[1,3]benzodioxolo[5,6-*c*]-1,3-dioxolo[4,5-*i*]phenanthridine*; **3**) *and (+)-11,13-Didehydro-11-deoxychelidonine* (=*(+)*-rel-*(12b*R*)-7,12b,13,14-Tetrahydro-13-methyl[1,3]benzodioxolo[5,6-*c*]-1,3-dioxolo[4,5-*i*]phenanthridine*; **4**). (±)-Corynoline ((±)-**1**) was isolated from *Corydalis incise* (Papaveraceae) [3]. To a soln. of **1** (100 mg) in abs. benzene (4 ml), $SOCl_2$ (0.2 ml) was added. The mixture was refluxed for 30 min. The solvent was evaporated and H_2O (10 ml) was added to the residue. The aq. soln. was adjusted to pH 10 with 28% aq. NH_3 soln. and extracted with Et_2O (2 × 25 ml). The Et_2O layer was dried (Na_2SO_4) and concentrated to a yellow-orange oil, which was subjected to column chromatography

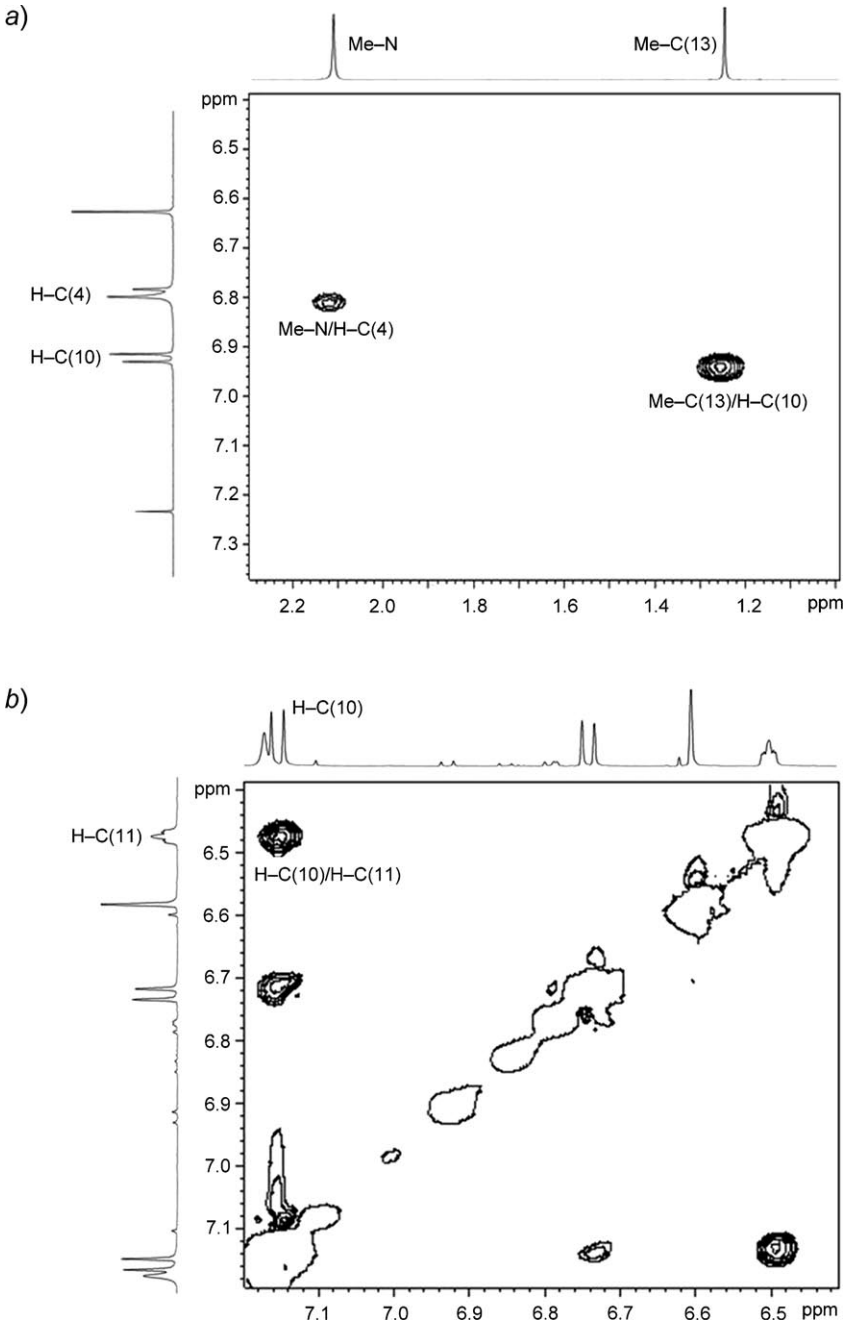

Fig. 3. *Partial NOESY plot of* a) **3** *and* b) **4**[1])

(Al_2O_3, benzene): **3** (64 mg). Prismatic crystals after recrystallization from $CHCl_3$/MeOH. M.p. 157.4–158.7°.

(+)-Chelidonine (**2**) was isolated from *Chelidonium majus* (Papaveraceae) [4]. Compound **4** was synthesized from **2** as described for **3**: **4** as prismatic crystals after crystallization from acetone/MeOH [7]. M.p. 170.4–171.9°.

X-Ray Crystal Analyses of **3** *and* **4**. A crystal was mounted on a nylon loop with 30% glycerol/mother liquor and then flash-frozen under a N_2 stream (120 K). Data collection was performed on a *CCD* diffractometer (*Bruker AXS SMART APEX*). The crystallographic data of **3** and **4** are given in *Table 1*. The crystal structure was solved by direct methods with the SIR92 program [16]. The positional parameters of the non-H-atoms were refined by a full-matrix least-squares method with anisotropic thermal parameters and the SHELXL-97 program [17], while those of the H-atoms were calculated on the basis of their configurational requirement. They were treated as riding with fixed isotropic displacement parameters ($U_{iso} = 1.2\ U_{eq}$ for the associated C- or N-atoms, or $U_{iso} = 1.5\ U_{eq}$ for O-atoms) and were not included as variables for the refinements. CCDC-724393 and 724392 contain the supplementary crystallographic data for **3** and **4**. These data can be accessed free of charge *via* http://www.ccdc.cam.ac.uk/data_request/cif.

NMR Measurement. ^{1}H- and ^{13}C-NMR Spectra: *Varian-VNMRS-500* (^{1}H at 499.7 MHz and ^{13}C at 125.7 MHz) spectrometer; at 23° and at a concentration of 0.04M in $CDCl_3$ soln; D resonance of $CDCl_3$ as the lock signal; chemical shifts δ with respect to the internal reference Me_4Si; signal assignments by gCOSY, NOESY, gHMBC, gHSQC, and DEPT, where the estimated standard deviations are 0.001 ppm for the chemical shift and *ca.* 0.5 Hz for the coupling constant *J*. The nuclear *Overhauser* enhancement and exchange spectroscopy (NOESY) plot was recorded in the phase-sensitive mode at 23° and with a mixing time of 700 ms.

REFERENCES

[1] H. Uemura, A. Takashima, K. Iwasaki, Y. Mukoyama, M. Kamigauchi, K. Tobetto, Jpn. Kokai Tokkyo Koho, 1999, pp. 13.
[2] M. Kamigauchi, Y. Noda, J. Nishijo, K. Iwasaki, K. Tobetto, Y. In, K. Tomoo, T. Ishida, *Bioorg. Med. Chem.* **2005**, *13*, 1867.
[3] C. Tani, N. Takao, *Yakugaku Zasshi* **1962**, *82*, 755.
[4] J. M. Probst, *Ann. Pharm.* **1839**, *29*, 113.
[5] V. Simanek, 'The Alkaloids', Ed. A. Brossi, Academic Press, New York, 1985, Vol. 26, pp. 185–234.
[6] N. Takao, M. Kamigauchi, K. Iwasa, N. Morita, K. Kuriyama, *Arch. Pharm.* **1984**, *317*, 223.
[7] N. Takao, *Chem. Pharm. Bull.* **1963**, *11*, 1306.
[8] M. H. Benn, R. E. Mitchell, *Can. J. Chem.* **1969**, *47*, 3701.
[9] T. M. Carlos, J. M. Harlan, *Blood* **1994**, *84*, 2068.
[10] D. Simmons, M. W. Makgoba, B. Seed, *Nature* **1988**, *331*, 624.
[11] L. Osborn, C. Hession, R. Tizard, C. Vassallo, S. Luhowskyj, G. Chi-Rosso, R. Lobb, *Cell* **1989**, *59*, 1203.
[12] N. Takao, N. Morita, M. Kamigauchi, K. Iwasa, K. Tomita, T. Fujiwara, S. Fujii, *Acta Crystallogr., Sect. B* **1981**, *37*, 2043.
[13] C. K. Johnson, ORTEP II, Report ORNL-5138, Oak Ridge National Laboratory, Oak Ridge Tennessee, 1976.
[14] M. Kamigauchi, Y. Noda, N. Takao, T. Ishida, M. Inoue, *Helv. Chim. Acta* **1986**, *69*, 1418.
[15] N. Takao, M. Kamigauchi, K. Iwasa, K. Tomita, T. Fujiwara, A. Wakahara, *Tetrahedron* **1979**, *35*, 1099.
[16] A. Altomare, M. C. Burla, M. Camalli, M. Cascarano, C. Giacovazzo, A. Guagliardi, G. Polidori, *J. Appl. Crystallogr.* **1994**, *27*, 435.
[17] G. M. Sheldrick, SHELXL97, Program for the Refinement of Crystal Structures, University of Göttingen, Göttingen, 1997.

Received June 9, 2009